Journal of Molecular Structure 1079 (2015) 383–390

Contents lists available at ScienceDirect

Journal of Molecular Structure

journal homepage: www.elsevier.com/locate/molstruc

Synthesis and dynamic stereochemistry of 4-aryl-thiomorpholine-3,5-dione derivatives

Joanna Szawkało [a], Jan K. Maurin [b,c], Franciszek Pluciński [b], Zbigniew Czarnocki [a,*]

[a] Faculty of Chemistry, University of Warsaw, Pasteura 1, 02-093 Warsaw, Poland
[b] National Medicines Institute, Chełmska 30/34, 00-725 Warsaw, Poland
[c] National Centre for Nuclear Research, 05-400 Otwock-Świerk, Poland

HIGHLIGHTS

- Seven new N-aryl-substituted thiomorpholine-3,5-diones have been characterized by X-ray diffraction method.
- Five *orto*-substituted N-aryl thiomorpholine-3,5-diones exhibited restricted rotations around N-aryl bond.
- Temperature-depended NMR and quantum chemical calculations were applied for the estimation of the energy barriers.

ARTICLE INFO

Article history:
Received 5 June 2014
Received in revised form 25 August 2014
Accepted 26 August 2014
Available online 3 September 2014

Keywords:
Imides
Atropisomerism
Heterocyclic compounds
Dynamic stereochemistry

ABSTRACT

A series of new N-aryl-substituted thiomorpholine-3,5-diones were synthesized. Crystal structures of seven compounds were established on the basis of X-ray crystallography. Stable at room temperature diastereomers were detected for (2-phenyl)-substituted derivatives using ^{1}H NMR. The dynamic stereochemistry of compound **36** was studied with variable-temperature ^{1}H NMR and the mechanism of diastereomers interconversion was proposed on the basis of quantum chemical calculations.

Introduction

The thiomorpholine-3,5-dione (3-thiaglutaric acid imide) structural motif is present in many pharmacologically active compounds. The synthesis of these derivatives was undertaken for evaluation as potentially useful hypnotics, sedatives and anticonvulsants [1–3]. Alkyl-substituted thiomorpholine-3,5-diones were found to have marked anticonvulsant activity against metrazol shock [2] and were considered as hypotensive agents [4]. More recently, these imides proved to be important pharmacophores in derivatives having antipsychotic [5], antimicrobial and antitumor activity [6]. From a chemical point of view, *N*-thiodiglicolyl derivatives of pharmacologically important glucosamine were found useful as glycosyl donors [7]. Relatively simple deprotonation of the methylene group in thiomorpholine-3,5-dione allows it subsequent alkylation giving rise to a variety of substituted structures [8]. The hydroxy or ethoxy lactams derived from thiazinediones undergo interesting intramolecular amidoalkylations giving efficient access to novel heterocyclic systems [9].

Despite its interesting and useful reactivity, the thiomorpholine-3,5-dione system has not yet been structurally evaluated and the Cambridge Crystallographic Database does not provide examples of compounds bearing this structural motif.

During our recent studies on potential antimicrobial agents, we turned our attention to selected thio- and thia-imides of dicarboxylic acids. Therefore in this work the synthesis as well as structural and spectroscopic studies of several new *N*-aryl-thiomorpholine-3,5-diones are presented.

Results and discussion

Synthesis of imides

The most straightforward and conventional method for preparation of cyclic imides is based on direct pyrolysis of the monoamide derived from a reaction of the corresponding anhydride and amine [10]. Acetic anhydride may also be used as dehydrating agent [11].

* Corresponding author. Tel.: +48 22 822 02 11; fax: +48 22 822 59 96.
E-mail address: czarnoz@chem.uw.edu.pl (Z. Czarnocki).

http://dx.doi.org/10.1016/j.molstruc.2014.08.046
0022-2860/

We have already found that BOP reagent [(benzotriazol-1-yloxy) tris(dimethyl-amino)phosphonium hexafluorophosphate, Castro reagent] may effectively be used at this step [12] and we applied this procedure to the synthesis of all described imides. Thus, the reaction of **1** with the corresponding aniline gave the mono-amide in quantitative yield which was then cyclized under mild conditions (BOP, THF, r.t.) to produce the desired imides in good yield (Scheme 1). The results are summarized in Table 1.

Crystallographic characterization of imides

In the case of compounds **29**, **30** and **33–37** we were able to obtain monocrystals suitable for X-ray experiments. Although molecules of all compounds were similar and contained the thioimide moiety linked through its nitrogen atom with a substituted phenyl ring, the crystal symmetry and crystal packing were different. The crystal and experimental parameters for all studied structures are compiled in Table 2. Structures can be divided at least into three different groups. The first one consists of structures of compounds **30**, **33** and **34**. The second one is formed by compounds **29** and **36** whereas the last one consists of structures of **35** and **37**. The first group formed by three monoclinic structures belonging to the $P2_1/c$ space group has a common feature which is a pair of centrosymmetric C(5)—H(5A)···O(2) hydrogen bonds between thioimide CH_2 fragments and respective carbonyl oxygen atoms.

*Structures of **30**, **33** and **34***

In Fig. 1 the crystal packing of **30** along the *b*-axis is shown.

The aforementioned dimers are additionally linked by series of weaker hydrogen bonds between phenyl ring H(11) hydrogen atoms and methoxy O(3) oxygens forming infinite dimeric zig-zag chains of molecules approximately in the 1 0 0 direction. Such chain is shown in Fig. 2.

The dimeric chains are additionally linked by C—H···O hydrogen bonds between H(9) phenyl hydrogen atoms and O(1) carbonyl oxygen atoms of the adjacent molecules.

Similar situation can be observed in the crystal structure of **33**. Although both unit cell parameters and the space group symmetry are very similar in these structures, the crystals are not isostructural. As before, molecules of **33** form infinite dimeric zig-zag chains but now, differently than in structure of **30**, the chains pass approximately in the 1 0 1 direction.

Table 1
Physical data and CCDC deposit numbers for imides **26–37**.

Imide	R	Mp (°C)	Yield (%)[a]	CCDC[c] Deposit no.
26	-H	211.5–213.0[b]	66	
27	-4-CH_3	205.5–207.0	88	
28	-2,5-diCH_3	137.0–138.0	59	
29	-4-NO_2	193.5–195.5	72	963,333
30	-4-OCH_3	196.0–197.0	77	963,336
31	-2-OCH_3	151.5–153.0	78	
32	-2,5-diOEt	94.5–95.5	77	
33	-3,4-O_2CH_2	217.0–218.0	72	963,337
34	-4-Cl	141.5–142.5	80	963,338
35	-2,4-diCl	144.0–146.0	90	963,335
36	-2,4-diF	160.0–161.0	97	963,334
37	-2-*t*Bu	172.5–174.0	78	963,339

[a] Based on compound **1**.
[b] Lit. [10] mp 214.5–215.5 °C.
[c] Cambridge Crystallographic Data Centre.

Different packing pattern was observed in the structure of **34**. Here also the hydrogen-bonded dimers are formed but they are linked *via* series of C(10)—H(10)···O(2) and C(7)—H(7)···O(2) intermolecular hydrogen bonds producing (1 0 0) double layers of molecules – highlighted in the center of the drawing in Fig. 3.

*Structures of **29** and **36***

In the second structural group, thioimide hydrogen atoms and carbonyl oxygens are also involved in C—H···O intermolecular hydrogen bonds but rather than forming centrosymmetric dimmers, they form infinite catemeric chains. In Fig. 4 the crystal packing of **29** molecules is shown along the *c*-axis.

The aforementioned catemeric chain is shown in Fig. 5. The molecules are related with twofold screw-axis symmetry in the 0 1 0 direction with the C(5)—H(52)···O(2) intermolecular hydrogen bonds. Additionally, translation-related molecules in the *b*-direction are linked with the C(12)—H(12)···O(1) bonds.

Apart from the above interactions, there are other weaker hydrogen bonds in the structure (not shown in the drawing) and involving other H-atoms and e.g. nitro group oxygens.

In the crystal structure of **36**, the thioimide methylene hydrogens and carbonyl oxygen atoms of the molecules are related by both *n*- and *a*-glide plane symmetry and are involved in a series of C(6)—H(6A)···O(1) and C(2)—H(2B)···O(2) hydrogen bonds formations. Additionally, molecules related by the twofold screw axes symmetry are hydrogen-bonded with the series of C(9)—H(9)···O(2)

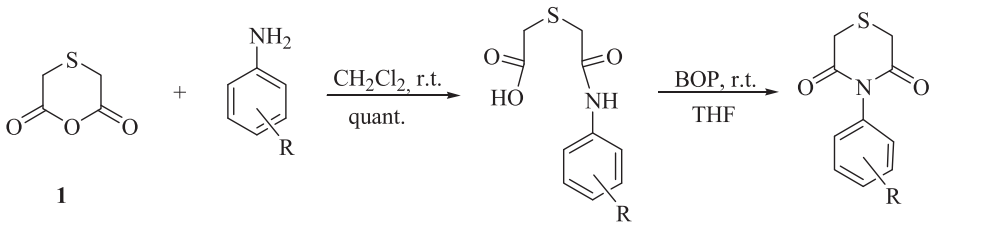

2 -H
3 -4-CH_3
4 -2,5-diCH_3
5 -4-NO_2
6 -4-OCH_3
7 -2-OCH_3
8 -2,5-diOC_2H_5
9 -3,4-O_2CH_2
10 -4-Cl
11 -2,4-diCl
12 -2,4-diF
13 -2-*t*Bu

14 -H
15 -4-CH_3
16 -2,5-diCH_3
17 -4-NO_2
18 -4-OCH_3
19 -2-OCH_3
20 -2,5-diOC_2H_5
21 -3,4-O_2CH_2
22 -4-Cl
23 -2,4-diCl
24 -2,4-diF
25 -2-*t*Bu

26 -H
27 -4-CH_3
28 -2,5-diCH_3
29 -4-NO_2
30 -4-OCH_3
31 -2-OCH_3
32 -2,5-diOC_2H_5
33 -3,4-O_2CH_2
34 -4-Cl
35 -2,4-diCl
36 -2,4-diF
37 -2-*t*Bu

Scheme 1. Synthesis of 3-thiaglutaric acid imides.

Table 2
Crystal data and structure refinement.

Identification code	**29**	**30**	**34**
Empirical formula	$C_{10}H_8N_2O_4S$	$C_{11}H_{11}NO_3S$	$C_{10}H_8ClNO_2S$
Crystal system	Monoclinic	Monoclinic	Monoclinic
Space group	*C2/c*	$P2_1/c$	$P2_1/c$
Unit cell dimensions	*a* = 20.6161(3) Å	*a* = 16.1404(2) Å,	*a* = 16.1139(8) Å
	b = 5.33630(10) Å, β = 116.267(2)°	*b* = 5.13560(10) Å, β = 101.3510(10)°	*b* = 5.1000(3) Å, β = 106.538(4)°
	c = 21.4366(3) Å	*c* = 13.6780(2) Å,	*c* = 13.6329(5) Å
Volume	2114.80(6) $Å^3$	1111.60(3) $Å^3$	1074.02(9) $Å^3$
Z	8	4	4
Goodness-of-fit on F^2	1.092	1.052	0.832
Final *R* indices [$I > 2\sigma(I)$]	*R*1 = 0.0347, *wR*2 = 0.1064	*R*1 = 0.0360, *wR*2 = 0.1096	*R*1 = 0.0380, *wR*2 = 0.0889
R indices (all data)	*R*1 = 0.0386, *wR*2 = 0.1087	*R*1 = 0.0380, *wR*2 = 0.1114	*R*1 = 0.0639, *wR*2 = 0.0961

Identification code	**33**	**36**	**35**	**37**
Empirical formula	$C_{11}H_9NO_4S$	$C_{10}H_7F_2NO_2S$	$C_{10}H_7Cl_2NO_2S$	$C_{14}H_{17}NO_2S$
Crystal system	Monoclinic	Orthorhombic	Orthorhombic	Monoclinic
Space group	$P2_1/c$	$Pna2_1$	*Pbca*	$P2_1/c$
Unit cell dimensions	*a* = 16.4661(7) Å	*a* = 13.70550(10) Å	*a* = 13.20240(10) Å	*a* = 14.06660(10) Å
	b = 5.1098(2) Å, β = 108.471(4)°	*b* = 5.49340(10) Å	*b* = 12.3947(2) Å	*b* = 13.88180(10) Å, β = 98.8120(10)°
	c = 13.5614(6) Å	*c* = 13.53920(10) Å	*c* = 14.43880(10) Å	*c* = 14.05910(10) Å
Volume	1082.25(8) $Å^3$	1019.36(2) $Å^3$	2362.76(5) $Å^3$	2712.91(3) $Å^3$
Z	4	4	8	8
Data/restraints/parameters	2014/0/154	1919/1/156	2254/0/145	5174/1/325
Goodness-of-fit on F^2	1.052	1.075	1.074	1.058
Final *R* indices [$I > 2\sigma(I)$]	*R*1 = 0.0455, *wR*2 = 0.1382	*R*1 = 0.0292, *wR*2 = 0.0846	*R*1 = 0.0429, *wR*2 = 0.1232	*R*1 = 0.0473, *wR*2 = 0.1457
R indices (all data)	*R*1 = 0.0576, *wR*2 = 0.1459	*R*1 = 0.0297, *wR*2 = 0.0850	*R*1 = 0.0490, *wR*2 = 0.1270	*R*1 = 0.0501, *wR*2 = 0.1489

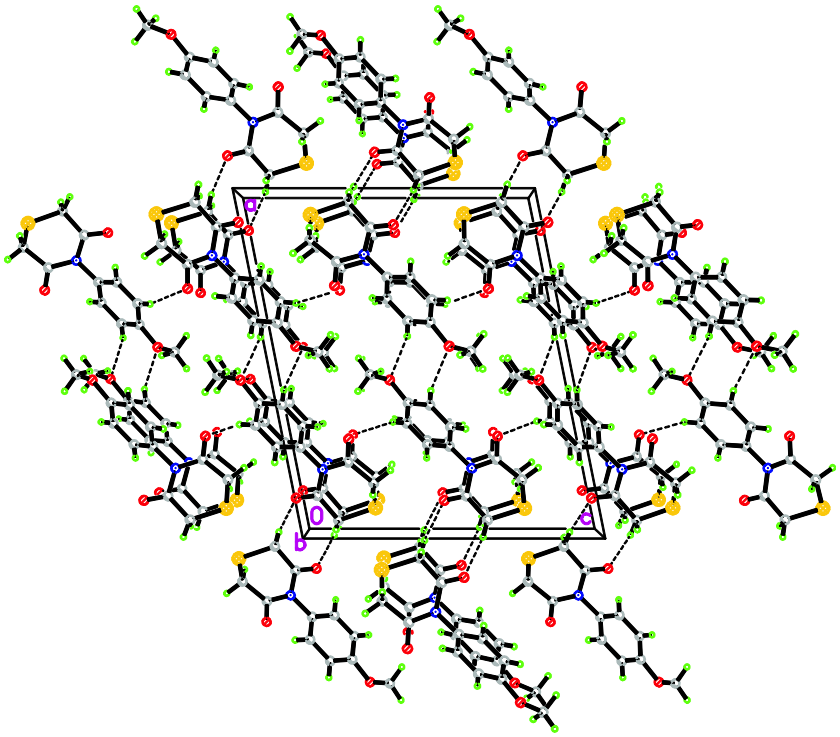

Fig. 1. The crystal packing of **30** shown along the *b*-axis. The C—H···O hydrogen bonds are shown as the dashed lines.

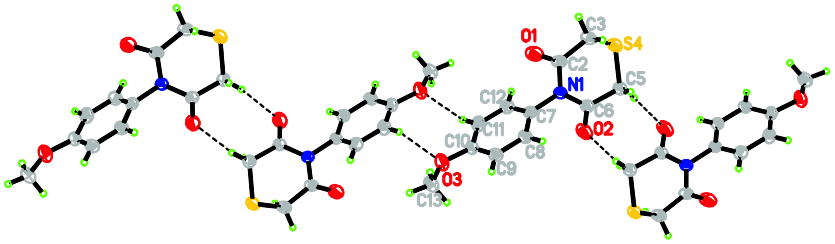

Fig. 2. The dimeric chain of molecules of **30**. The non-H atoms are shown as 30% probability ellipsoids.

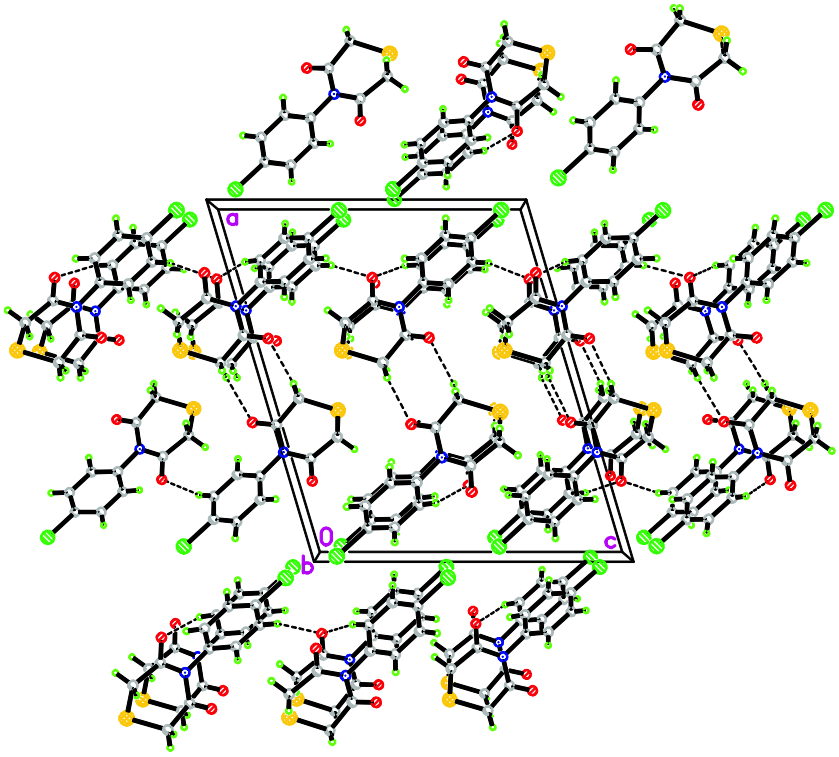

Fig. 3. The crystal packing of **34** shown in the *b*-direction.

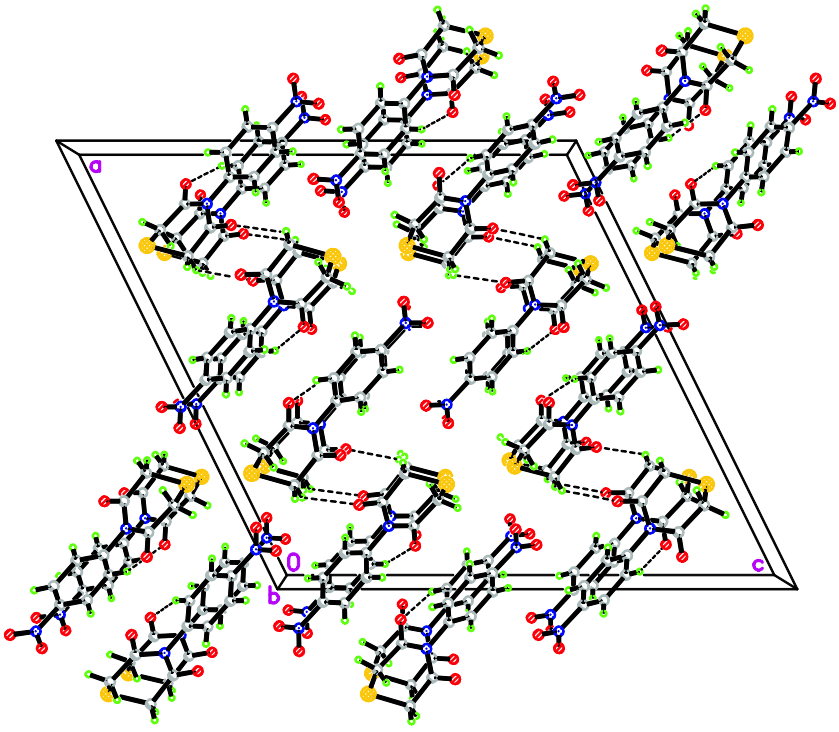

Fig. 4. Crystal packing in the structure of **29**. The C—H···O hydrogen bonds are shown as the dashed lines.

bonds. The three-dimensional hydrogen bonds system is completed with C(11)—H11···O(2) bonds.

*Structures of **35** and **37***

In the last group no relatively strong H-bonds involving thioimide CH_2 hydrogen atoms are observed. Instead, hydrogen atoms of the activated phenyl rings are involved in hydrogen bonds formation between molecules related by the glide planes symmetry (Fig. 6).

In this crystal structure series of C(9)—H(9)···O(1) and C(11)—H(11)···O(1) hydrogen bonds could be seen. One can notice chain structures involving e.g. molecules related by the *a*-glide plane symmetry. Such chain is shown below in Fig. 7.

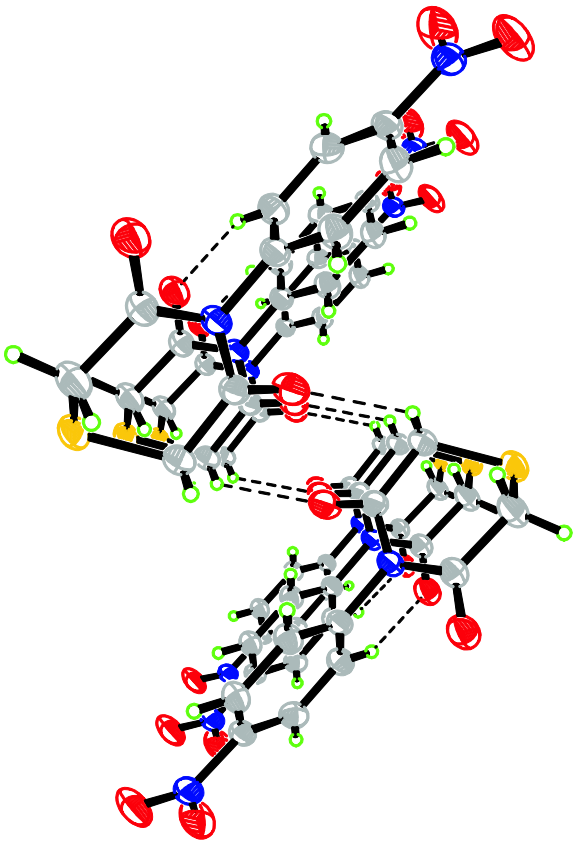

Fig. 5. The catemeric chain of molecules in the structure of **29**. The non-hydrogen atoms are shown as 30% probability ellipsoids. Hydrogen bonds are shown as the dashed lines.

Independent part of the unit cell of **37** is composed of two, slightly differing in geometry, molecules. Molecule B is partly disordered in its *t*-butyl substituent (Fig. 8).

Molecules are linked together in chains by weak C—H···O hydrogen bonds (Fig. 9).

The neighboring chains are additionally linked with pairs of intermolecular centrosymmetric dimeric C16A—H16A···S1A bonds.

Hydrogen bonds geometry

In Table 3 the geometry of potential C—H···O interactions observed in the crystal structures of imides are summarized. The idea of weak hydrogen bonds, where a carbon atom acts as a donor, are generally accepted by crystallographic community starting from the important work of Taylor and Kennard (1982) [13], in which, basing on the neutron diffraction data the directionality of the C—H···O interaction was detected and revealed that some H···O distances were significantly shorter than the sum of the van der Waals distances (2.4 Å). These two features make the C—H···O interactions similar to that of O—H···O hydrogen bonds. The hydrogen bonds investigated by Taylor and Kennard were strong C—H···O bonds with the most frequently observed bond angles of 150–160° [14]. The interactions observed in reported here structures might be considered as weak or medium-strong C—H···O hydrogen bonds, although the bond length criterion of the bond strength is often misleading [14,15]. In some cases other factors e.g. steric repulsion operate, as in the case of compound **37** where they prevent the formation of C—H···O bonds between thioimide C—H and carbonyl oxygens from the neighboring molecules.

NMR spectroscopy (in solution) and computational analysis

The ^{1}H NMR spectra of compounds **29**, **33** and **34** have relatively simple structure due to the symmetry of molecules. In all cases signals corresponding to methylene protons in the heterocyclic part of the molecule appear as singlets at approx 3.70 ppm. Only in the case of compound **29**, this signal is shifted to 3.73 ppm reflecting the electron-withdrawing effect of the nitro group. The resonance of the aromatic protons appears as group of multiplets at 6.50–7.50 ppm. The ^{13}C NMR spectra were also simplified due to the symmetry of molecules and the signal corresponding to C-3 carbon atom is located at approx. 32 ppm whereas the C=O group resonance is observed at approx. 168 ppm.

The ^{1}H NMR spectra of compounds **28**, **31**, **32**, **35–37** showed more interesting features. The presence of *ortho*-substituent at the phenyl ring apparently caused a restricted rotation around the C—N bond resulting in diastereotopicity (at least at the NMR time scale) of the methylene protons at C-3. As a consequence, the signal at approximately 3.60 ppm splits into two doublets of ca. J_{gem} = 17 Hz. The effect of hindered rotation and non-planar

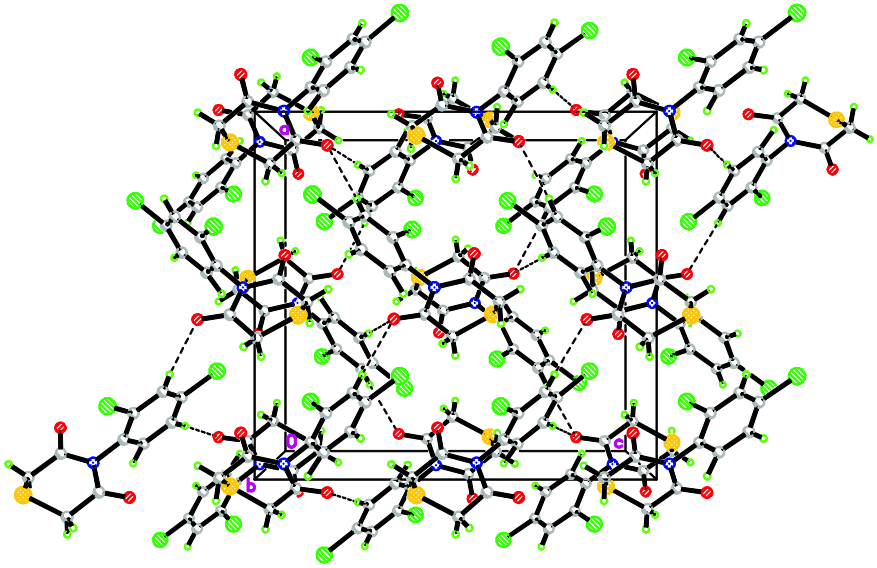

Fig. 6. Crystal packing in **35** shown along *b*-direction. The C—H···O hydrogen bonds are shown as dashed lines.

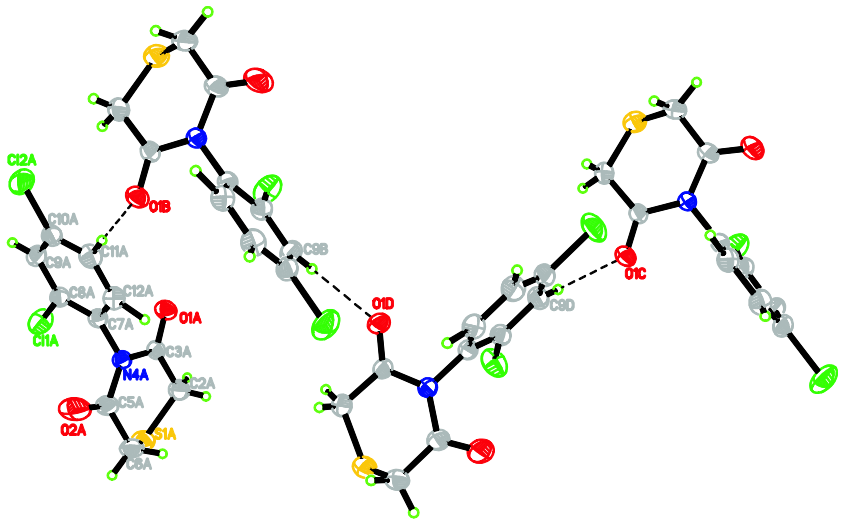

Fig. 7. Hydrogen-bonded chain of molecules formed by series of C(9)—H(9)···O(1) hydrogen bonds. The non-hydrogen atoms are shown as 30% probability ellipsoids.

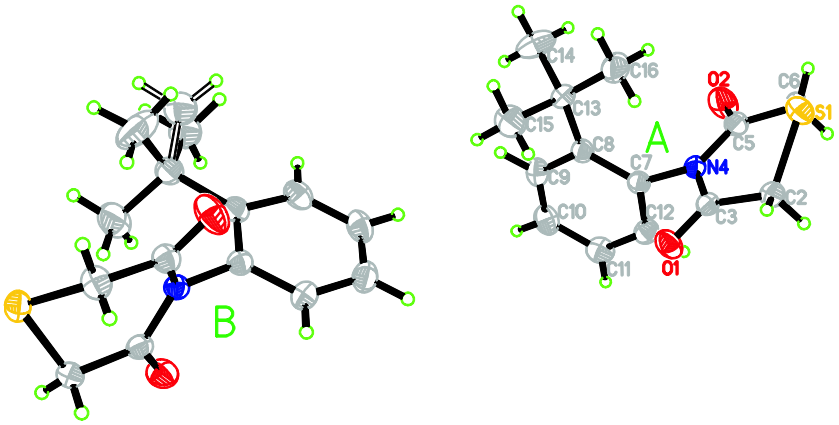

Fig. 8. Independent part of the unit cell of the structure of **37**. The non-H atoms are shown as the 30% probability ellipsoids. Atom C(15) from the molecule B is partly disordered.

conformations about the C—N bond in aryl-imides has already been documented by several authors [16,11]. The dynamic ^{1}H NMR study of rotational energy barrier provided valuable information concerning conformer interconversion [17]. In the case of compounds **28**, **31**, **32**, and **35**–**37**, possible isomerization of diastereomers might be caused by two distinct mechanisms. According to the first one, the diastereomers may interconvert due to a conformational change taking place in the heterocyclic part of the molecule as shown in Fig. 10 for compound **37**.

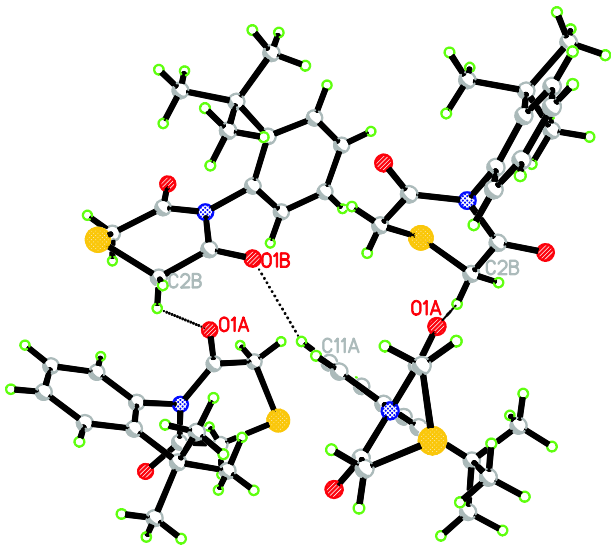

Fig. 9. The H-bonded chain of molecules passing along the *c*-direction. The consecutive A and B molecules in the chain are related by a *c*-glide plane symmetry.

Alternatively, the same result might be obtained *via* the rotation around N-aryl bond. In order to estimate the energy requirements for both processes, we initially calculated the activation energy for the conformational change involving the heterocyclic part of the molecule. This calculation was done only for **36** since the thioimide ring is the part of all studied compounds and due to that its inversion energy is expected to be similar. The obtained value of energy of the thioimide ring inversion was 6.0 kcal/mol. This energy value suggests rather unrestricted conformational changes in the heterocyclic part.

In order to estimate the energy requirements for the alternative mechanism involving the N—C_{aryl} bond rotation, we performed a set of additional calculations. The results are given in Table 4.

As shown in Table 4, the rotation around the N—C_{aryl} bond is a medium-energy process except for compound **37**, in which the rotation is stopped. The calculations were done by *ab initio* DFT method with the implemented B3LYP electron density functional and 6-31G* function basis [18]. After geometry optimization of the initial structures, their rotation energy profiles were determined as the result of rotation of the aryl substituent around

Table 3
C—H···O hydrogen bonds geometry (Å and °).

Compound	D—H···A	Distances			<(DHA)	Symmetry operations generating equivalents[a]
		D—H	H···A	D···A		
29	C(12)—H(12)···O(1)[1)]	0.93(2)	2.49(2)	3.381(2)	159.5(17)	[1)] $x, y+1, z$
	C(5)—H(52)···O(2)[2)]	0.93(2)	2.56(2)	3.268(2)	133.2(17)	[2)] $-x+1/2, y-1/2, -z+1/2$
	C(9)—H(9)···O(4)[3)]	0.91(2)	2.62(2)	3.331(3)	135.8(17)	[3)] $-x, -y-1, -z$
	C(5)—H(52)···O(4)[4)]	0.93(2)	2.65(2)	3.304(2)	128.4(17)	[4)] $x+1/2, -y-1/2, z+1/2$
30	C(5)—H(5A)···O(2)[1)]	0.97(3)	2.33(3)	3.293(2)	171(2)	[1)] $-x+2, -y, -z+1$
	C(9)—H(9)···O(1)[2)]	0.91(2)	2.57(2)	3.452(2)	162.2(17)	[2)] $x, -y+11/2, z+1/2$
	C(11)—H(11)···O(3)[3)]	0.96(2)	2.52(2)	3.430(2)	158.3(18)	[3)] $-x+1, -y, -z+1$
34	C(3)—H(31)···O(1)[1)]	0.94(3)	2.41(3)	3.308(4)	158(3)	[1)] $-x+1, -y+1, -z+1$
	C(10)—H(10)···O(2)[2)]	0.94(3)	2.47(3)	3.393(4)	166(3)	[2)] $x, -y+21/2, z-1/2$
	C(7)—H(7)···O(2)[3)]	0.89(3)	2.58(3)	3.432(4)	160(3)	[3)] $x, y-1, z$
33	C(6)—H(6B)···O(2)[1)]	0.88(4)	2.44(4)	3.302(4)	167(3)	[1)] $-x+1, -y+1, -z$
	C(8)—H(8)···O(1)[2)]	0.87(3)	2.63(3)	3.446(3)	156(2)	[2)] $x, y-1, z$
	C(13)—H(13A)···O(4)[3)]	1.08(4)	2.49(4)	3.250(4)	126(3)	[3)] $-x, -y+1, -z-1$
	C(13)—H(13B)···O(3)[4)]	1.20(4)	2.69(4)	3.178(5)	103(2)	[4)] $-x, y+1/2, -z-1/2$
	C(13)—H(13B)···O(1)[5)]	1.20(4)	2.69(4)	3.674(4)	138(2)	[5)] $-x, y-1/2, -z-1/2$
36	C(6)—H(6A)···O(1)[1)]	0.82(4)	2.62(4)	3.259(3)	136(3)	[1)] $-x+1/2, y+1/2, z-1/2$
	C(11)—H(11)···O(1)[2)]	1.05(3)	2.43(3)	3.472(3)	172(2)	[2)] $x-1/2, -y+1/2, z$
	C(2)—H(2B)···O(2)[3)]	0.92(3)	2.61(3)	3.178(2)	121(2)	[3)] $x+1/2, -y+11/2, z$
	C(9)—H(9)···O(2)[4)]	0.95(3)	2.54(3)	3.374(2)	146(2)	[4)] $-x, -y+2, z+1/2$
35	C(9)—H(9)···O(1)[1)]	0.89(3)	2.52(3)	3.383(3)	165(3)	[1)] $x-1/2, y, -z+1/2$
	C(11)—H(11)···O(1)[2)]	0.91(3)	2.40(3)	3.309(3)	178(3)	[2)] $-x, y+1/2, -z+1/2$
37	C(2B)—H(2B1)···O(1A)[1)]	0.89(3)	2.59(3)	3.201(3)	126(2)	[1)] $-x+1, y-1/2, -z-1/2$
	C(11A)—H(11A)···O(1B)[2)]	0.93	2.68	3.348(3)	129.5	[2)] $-x+1, -y+2, -z-1$

[a] The numbers correspond to the respective structures.

Table 4
The energy of rotational barrier of imides **28**, **31**, **32**, **35–37**.

Imide	Substituents	Energy of rotational barrier (kcal/mol)
28	-2,5-diCH_3	50.2
31	-2-OCH_3	8.1
32	-2,5-diOEt	12.4
35	-2,4-diCl	17.1
36	-2,4-diF	13.6
37	-2-*t*Bu	100.9

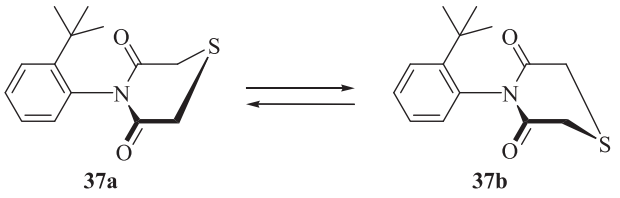

Fig. 10. Diastereomers of **37** resulting from conformational change of 3,5-thiomorpholine-3.5-dione ring.

N—C bond by 180°. This rotation range was divided into ten even angular steps and on each of them the energy of the molecule was calculated after its prior geometry optimization.

We also performed variable temperature ^{1}H NMR experiments on compound **36** observing changes in signals corresponding to protons at C-2 and C-6 positions of the heterocycle. The results seen in Fig. 11 indicate the temperature dependence of the signals.

The signals observed at 25 °C were found to become closer as the temperature was raised, and coalesced at 120 °C. These NMR spectra may be considered as AB spin system only slightly perturbed toward AA′BB′ one. The activation energy of 19.7 kcal/mol has been then calculated for the conformational interconversion of atropisomers with the help of Eyring's equation.

$$\Delta G = aT_c\left[10.319 + \log\left(\frac{T_c}{k}\right)\right]$$

where $a = 4.575 \times 10^{-3}$ for units of kcal/mol, T_c and k denote coalescence temperature and the rate constant of isomerisation $k = \frac{\pi\sqrt{(\nu_A-\nu_B)^2+6J_{AB}^2}}{\sqrt{2}}$. Parameters ν_A, ν_B and J_{AB} stand for: chemical shift of proton A, chemical shift of proton B and coupling constant between proton A and B in AB spin system, respectively. The calculated values are: $\nu_A - \nu_B$ = 12.8 Hz and J_{AB} = 16.0 Hz. For simplification, the AB spin system was assumed in the calculation. This form of the Eyring's equation was chosen assuming that the populations of both isomers are the same and the observed protons in the NMR spectrum being in structurally equivalent positions form an AB spin system. In the case of compound **36** it refers to equatorial and axial protons in 2 and 6 positions in the thioimide ring.

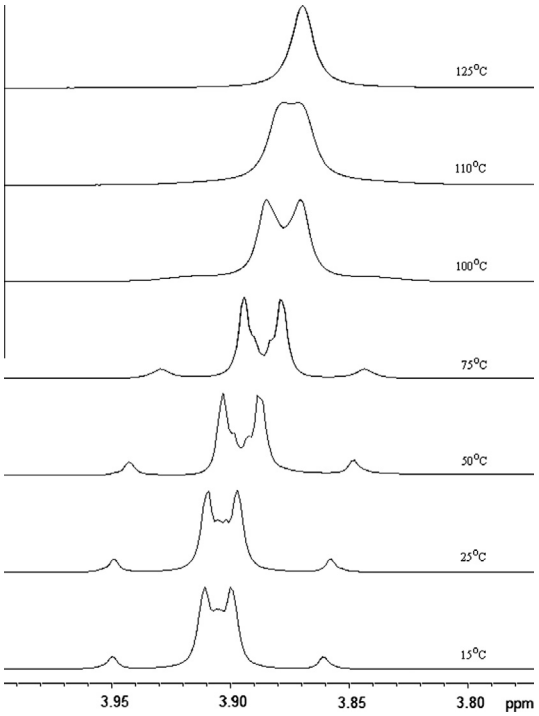

Fig. 11. Dynamic ^{1}H NMR experiment on compound **36**.

These both types of protons form an AB spin system slightly deviated toward AA′BB′ which degenerates into A_2 one at the coalescence temperature. The difference in the experimental (19.7 kcal/mol) and theoretical (13.6 kcal/mol) value of the rotation barrier for compound **36** may be attributed to the solvent (DMSO) effect that is difficult to incorporate in the calculations. Nevertheless, the energy calculation seems to be a useful tool for a preliminary estimation of the dynamic stereochemistry of conformationally mobile molecules.

Similar experiment of temperature-dependent NMR was performed for compound **37**, for which quantum chemical calculations predicted blocking the rotation of the phenyl ring. As expected, the coalescence of the signals of protons at the positions 2 and 6 in the thioimide ring (AB spin system) was not observed up to 185 °C illustrating the existence of an intrinsic anisochrony of the system [19].

Conclusions

In a search for novel antibacterial compounds possessing sulfur heterocyclic motif, we prepared a series of new *N*-aryl-substituted thiomorpholine-3,5-diones. The structures of seven compounds were established on the basis of X-ray crystallography. In the case of (2-phenyl)-substituted derivatives, diastereomers stable at room temperature were detected in ^{1}H NMR. The dynamic stereochemistry of compound **36** was subjected to a more detailed study with variable-temperature ^{1}H NMR observing changes in signals corresponding to protons at C-2 and C-6 positions of the heterocycle. On the basis of detected coalescence temperature, the energy barrier to rotation was calculated and this value was compared with the calculated one. The mechanism of diastereomers interconversion was proposed on the basis of quantum chemical calculations.

Experimental

The NMR spectra were recorded on a Varian Unity Plus spectrometer operating at 200 MHz or at 500 MHz for ^{1}H NMR and at 50 MHz or at 125 MHz for ^{13}C NMR. The spectra were measured in $CDCl_3$ or DMSO-d_6 and are given as δ values (in ppm) relative to TMS. Mass spectra were collected on Quattro LC Micromass and LCT Micromass TOF HiRes apparatus with ESI+ or ESI- ionization. Melting points were determined with EZ-Melt melting point apparatus and were uncorrected. TLC analyses were performed on silica gel plates (Merck Silica Gel 60 F254) and visualized using UV-light or in iodine vapors. Column chromatography was carried out at atmospheric pressure using Silica Gel 60 (230–400 mesh, Merck). Solvents used in the reactions were anhydrous. CH_2Cl_2 was dried with anhydrous $CaCl_2$. THF was dried with CaH_2 and distilled under argon directly before the reaction. BOP and all other reactants were purchased from Sigma–Aldrich. Anhydride **1** was prepared according to literature protocol [20]. The single-crystal X-ray measurements were carried out on Oxford Diffraction Xcalibur R κ-axis diffractometer with CCD Ruby detector. In all cases, Cu Kα characteristic radiation was applied. After initial corrections and data reduction, intensities of reflections were used to solve and consecutively refine structures using SHELXS97 and SHELXL97 programs [21].

*General method for synthesis of imides **26–37***

Anhydride **1** (100 mg, 0.757 mmol) was dissolved in a minimal amount of dry CH_2Cl_2 and corresponding aniline **2–13** (1 eq) was added in dry CH_2Cl_2. The solution was stirred for 24 h at room temperature. The solvent was evaporated and the monoamides **14–25** were air-dried, and used without further purification.

Appropriate monoamide (**14–25**) (0.5 mmole) was dissolved in dry, freshly distilled THF (10 ml) at room temperature under argon. BOP (1.05 eq) was added to the mixture followed by the solution of triethylamine (TEA) (0.5 ml) in THF (1 ml). The reaction mixture was then stirred at room temperature for 20 min and another portion of BOP (0.5 eq) was added. After 40 min the solvent was evaporated. The residue was dissolved in $CHCl_3$ and washed with 10% citric acid solution, sat. Na_2CO_3 solution, water and brine. Combined organic layers were dried over $MgSO_4$, filtered and evaporated to dryness. Imides **26–37** were purified by column chromatography on silica gel using mixture hexan/EtOAc (0–15% v/v) as eluent. Yields are listed in Table 1.

Appendix A. Supplementary material

Supplementary data associated with this article can be found, in the online version, at http://dx.doi.org/10.1016/j.molstruc.2014.08.046.

References

[1] M. Babu, K. Pitchumani, P. Ramesh, Bioorg. Med. Chem. Lett. 22 (2012) 1263–1266.
[2] Ch. Barkenbus, P. Panzera, J. Org. Chem. 20 (1955) 237–243.
[3] (a) G.S. Skinner, J.B. Bicking, J. Am. Chem. Soc. 76 (1954) 2776–2780; (b) G.S. Skinner, R.N. Macnair, J. Org. Chem. 25 (1960) 1164–1168.
[4] F. Fried, R.N. Prasad, A.P. Gaunce, J. Med. Chem. 10 (1967) 279–281.
[5] J.S. New, W.L. Christopher, J.P. Yevich, R. Butler, R.F. Schlemmer, C.P. VanderMaelen, J.A. Cipollina, J. Med. Chem. 32 (1989) 1147–1156.
[6] (a) M.M. Ghorab, M.S.A. El Gaby, N.E. Amin, N.M.H. Taha, M.A. Shehab, I.M.I. Faker, Phosphorus, Sulfur Silicon Relat. Elem. 183 (2008). 2929-1942; (b) T.M. Abdel-Rahman, J. Heterocycl. Chem. 43 (2006) 527–534.
[7] J.C. Castro-Palomino, R.R. Schmidt, Tetrahedron Lett. 41 (2000) 629–632.
[8] J.F. Wolfe, T.G. Rogers, J. Org. Chem. 35 (1970). 3600–3007.
[9] (a) P.N.W. van der Vliet, J.A.M. Hamersma, W.N. Speckamp, Tetrahedron 41 (1985) 2007–2014; (b) M.S. Hadley, F.D. King, R.T. Martin, Tetrahedron Lett. 24 (1983) 91–94.
[10] R.A. Aitken, D.M.M. Farrell, E.H.M. Kirton, Chem. Heterocycl. Comp. 37 (2001) 1526–1531.
[11] D.J. Bennett, A.J. Blake, P.A. Cooke, C.R.A. Godfrey, P.L. Pickering, N.S. Simpkins, M.D. Walker, C. Wilson, Tetrahedron 60 (2004) 4491–4511.
[12] (a) Z. Czarnocki, I. Matuszewska, M. Matuszewska, Org. Prep. Proced. Int. 30 (1998) 699–702; (b) K.K. Krawczyk, D. Madej, J.K. Maurin, Z. Czarnocki, C. R. Chim. 15 (2012) 384–388.
[13] R. Taylor, O. Kennard, J. Am. Chem. Soc. 104 (1982) 5063–5070.
[14] T. Steiner, Chem. Commun. (1997) 727–734.
[15] G.R. Desiraju, T. Steiner, "The weak Hydrogen Bond" IUCR Monographs on Crystallography 9, Oxford University Press, Oxford, 1999.
[16] (a) S.M. Verma, N.B. Singh, Aust. J. Chem. 29 (1976) 295–300; (b) K. Kondo, T. Iida, H. Fujita, T. Suzuki, R. Wakabayashi, K. Yamaguchi, Y. Murakami, Tetrahedron 57 (2001) 4115–4122; (c) M.T. Maghsoodlou, G. Marandi, S.M.H. Khorassani, L. Saghatforoush, A. Aminkhani, R. Kabiri, Indian J. Chem. 47B (2008) 1151–1153.
[17] M. Oki, in: Application of Dynamic NMR Spectroscopy to Organic Chemistry, VCH Publishers, 1985.
[18] Wavefunction Inc, Spartan '08.
[19] H. Günther, NMR Spectroscopy, second ed., Wiley, New York, 1995 (chapter 9).
[20] Y. Nagao, S. Miyamoto, K. Hayashi, A. Mihira, S. Sano, Tetrahedron Lett. 43 (2002) 1519–1522.
[21] .G.M. Sheldrick, Acta Crystallogr., Sect. A 64 (2008) 112–122.